Published in final edited form as:
Nucl Med Biol. 2010 February ; 37(2): 205–214. doi:10.1016/j.nucmedbio.2009.10.007.

High Resolution Imaging of Brain 5-HT$_{1B}$ Receptors in the Rhesus Monkey using [^{11}C]P943

Nabeel Nabulsi[1,*], **Yiyun Huang**[1], **David Weinzimmer**[1], **Jim Ropchan**[1], **James J Frost**[1], **Timothy McCarthy**[2], **Richard E Carson**[1], and **Yu-Shin Ding**[1]

[1]Yale PET Center, Department of Diagnostic Radiology and Psychiatry, Yale University School of Medicine, New Haven, CT 06520

[2]Pfizer Global R&D, Groton, CT 06340

Abstract

The serotonin 5-HT$_{1B}$ receptors regulate the release of serotonin and are involved in various disease states, including depression and schizophrenia. The goal of the study was to evaluate a high affinity and high selectivity antagonist, [^{11}C]P943, as a PET tracer for imaging the 5-HT$_{1B}$ receptor. [^{11}C]P943 was synthesized via *N*-methylation of the precursor with [^{11}C]methyl iodide or [^{11}C]methyl triflate using automated modules. The average radiochemical yield was approx. 10% with radiochemical purity of >99% and specific activity of 8.8 ± 3.6 mCi/nmol at the end-of-synthesis (n = 37). PET imaging was performed in non-human primates with a High Resolution Research Tomograph (HRRT) scanner with a bolus/infusion paradigm. Binding potential (BP_{ND}) was calculated using the equilibrium ratios of regions to cerebellum. The tracer uptake was highest in the globus pallidus and occipital cortex, moderate in basal ganglia and thalamus, and lowest in the cerebellum, which is consistent with the known brain distribution of 5-HT$_{1B}$ receptors. Infusion of tracer at different specific activities (by adding various amount of unlabeled P943) reduced BP_{ND} values in a dose-dependent manner, demonstrating the saturability of the tracer binding. Blocking studies with GR127935 (2 mg/kg, IV), a selective 5-HT$_{1B}$/5-HT$_{1D}$ antagonist, resulted in reduction of BP_{ND} values by 42-95% across regions; for an example, in occipital region from 0.71 to 0.03, indicating a complete blockade. These results demonstrate the saturability and specificity of [^{11}C]P943 for 5HT$_{1B}$ receptors, suggesting its suitability as a PET radiotracer for in vivo evaluations of the 5-HT$_{1B}$ receptor system in humans.

Keywords

5-HT$_{1B}$ receptor; antagonist; PET; radioligand; C-11; HRRT

1. Introduction

Functional abnormalities of the 5-HT system have been linked to a variety of psychiatric disorders, including anxiety [1,2,3] depression [4], and schizophrenia [5,6]. The serotonin 5-HT$_{1B}$ receptors, located on the 5-HT neurons, are autoreceptors involved in the regulation of synaptic 5-HT concentrations [7]. As a result, these receptors are a target for pharmaceutical

Corresponding Author: Yu-Shin Ding, Ph.D., Professor of Diagnostic Radiology, Director, Radiochemistry R&D, Co-director, Yale PET Center, P.O. Box 208048, New Haven, CT 06520-8048, Tel: (203)785-4297, Fax: (203)785-3107.
*Current address: Kreitchman PET Center, Columbia University Medical Center, New York, NY.

development for their potential in the treatment of multiple psychiatric disorders, including anxiety, depression and substance abuse [8,9,10,11]. It has been suggested that selective blocking of the 5-HT_{1B} receptors in the brain could pave the way for a novel approach for managing psychiatric disorders [6,12]. For example, in animal models, blockade of the terminal 5-HT_{1B} receptors with an antagonist has been demonstrated to increase synaptic 5-HT concentration [13, 14]. In light of these observations, 5-HT_{1B} antagonists, either alone or in combination with selective serotonin reuptake inhibitors (SSRIs), may hold potential as rapid-onset antidepressants. Thus, imaging the 5-HT_{1B} receptors in vivo will aid in the elucidation of 5-HT_{1B} receptor functions, and in the development of novel antidepressants.

P943, R-1-[4-(2-methoxy-isopropyl)-phenyl]-3-[2-(4-methyl-piperazin-1-yl)benzyl]-pyrrolidin-2-one, is a potent 5-HT_{1B} antagonist in vitro, which binds with high affinity to the human 5-HT_{1B} receptor expressed in HeLa cells (K_i = 0.77 nM). The affinity of P943 for other 5-HT and non-5-HT receptors is at least 100-fold lower, making this a highly 5-HT_{1B}-selective ligand (e.g. K_I = 85 nM for 5-HT_{1A} receptors) [15,16].

Its specificity and selectivity was characterized by in vitro autoradiography studies, showing localization of radioactivity in regions known to contain high levels of the 5-HT_{1B} receptor (e.g. globus pallidus and substantia nigra). Specific binding to these slices was demonstrated by co-incubation of the radiotracer with 10 μM serotonin. No specific accumulation was observed in the cerebellum, a region known to be devoid of $5HT_{1B}$ receptors. Specific displacement of the radiotracer was achieved using a structurally unrelated, but selective 5-HT_{1B} inhibitor (CP-448,187). Its antagonist disposition was demonstrated in vitro in guinea pig substantia nigra, by blocking the reduction of 5-HT_{1B} agonist-induced adenylate cyclase activities. The enantioselectivity of P943 has also been shown via ex vivo autoradiography studies in guinea pig [15,16]. The details of these in vitro and in vivo screening and comparative studies will be published elsewhere. A summary of the in vitro pharmacology profile for unlabeled P943, which was performed by the NIMH Psychoactive Drug Screening Program, is shown in Table 1, demonstrating its potency and selectivity towards $5HT_{1B}$ receptors.

The aim of the present study was to carry out pre-clinical evaluation of [^{11}C]P943 in non-human primates with the high resolution research tomography (HRRT) PET scanner. For initial quantitative evaluation, the binding potential (BP_{ND}) was calculated using the equilibrium ratios of regions to cerebellum, assuming this region is devoid of 5-HT_{1B} receptors. The saturability and specificity of the tracer binding was assessed by blocking studies with unlabeled parent compound and GR127935 (a selective 5-HT_{1B}/5-HT_{1D} antagonist). Here we report the preparation of [^{11}C]P943 and its evaluation in non-human primates to assess its in vivo characteristics.

2. Materials and Methods

2.1. General

Reagents and solvents were purchased from the standard commercial sources, i.e., Sigma-Aldrich, Fisher Scientific, Merck or J. T. Baker, and were used without purification. Both the P943 standard and the *N*-desmethyl-precursor were provided by Pfizer, Inc.

Synthesis of [^{11}C]P943 was carried out either with a TRACERLab™ F × C automated synthesis module (GE Medical Systems), or with a AutoLoop™ (Bioscan Inc., Washington, D.C.). For the F × C module, the radioligand was purified by a preparative HPLC system that is included with, and integrated into, the module. It consists of a *Syknm* solvent delivery system, injection valve, and a radioactivity flow-through detector operating in series with a UV detector (254 nm). The latter is a *WellChrom* Filter-Photometer K2001 with deuterium

lamp containing 4 wavelength filters: 200, 220, 254 and 280 nm. For the AutoLoop, a KNAUER UV detector (254 nm) was used, operating in series with the AutoLoop's gamma-detector that is included within the product module, along with a Shimadzu LC-20AT solvent delivery system.

For both synthesis modules, the purification of the product was achieved by using a semi preparative HPLC column (Phenomenex's Luna C18(2), 10μ, 250 × 10 mm). The column was eluted under isocratic conditions with a mobile phase composed of 40:60 (v/v) acetonitrile/0.1 M ammonium acetate buffer of pH 5.5 (with acetic acid) and a flow rate of 5 mL/min.

2.2. Radiochemistry

2.2.1. Synthesis and formulation of (R)-1-(4-(2-methoxypropan-2-yl)phenyl)-3-(2-(4-methylpiperazin-1-yl)benzyl)pyrrolidin-2-one ([^{11}C]P943)—

Radioisotope C-11 carbon dioxide ([^{11}C]CO_2) was produced by the ^{14}N(p,α)^{11}C nuclear reaction with the PETtrace cyclotron (GE Medical Systems) using 16.5 ± 0.1 MeV proton irradiation (40 min, 55 mA) of nitrogen gas containing 0.5% oxygen. C-11 methyl iodide ([^{11}C]CH_3I) was synthesized from [^{11}C]CO_2 using a GE MeI Microlab®. Briefly, [^{11}C]CO_2 was reduced by hydrogen with a Ni catalyst to C-11 methane ([^{11}C]CH_4) followed by a gas phase reaction with iodine to form [^{11}C]CH_3I [17], which was then delivered to either the AutoLoop module or the FxC module for incorporation.

a. Synthesis using the FxC Module: [^{11}C]CH_3I (from the MicroLab) was swept through the silver triflate column [18,19] at 190° C, and the resulting [^{11}C]methyl triflate was bubbled into a solution of desmethyl P943 (1 mg) in 400 mL of anhydrous dimethylformamide (DMF) cooled at -30° C until activity peaked. The resulting solution was then heated at 100° C for 4 minutes. The reaction mixture was cooled down to 80° C, then diluted with 1.3 mL of de-ionized water and injected onto the semi preparative HPLC column. The radioactivity fraction eluting between 10-12 min was collected, diluted with 50 mL of water, and loaded onto a Waters Classic C18 Sep-Pak cartridge. The Sep-Pak was rinsed with 10 mL of 1 mM HCl, then eluted with 1 mL of USP absolute ethanol (Pharmco, USP) into the FxC's intermediate product vessel that contained a stirring mixture of 7 mL saline (USP, American Regent) and 40 uL of 4.2% sodium bicarbonate (Abraxis, sterile, preservative & pyrogen free). The Sep-Pak was further eluted with 3 mL of saline. Then the resulting solution mixture from the intermediate product vessel was passed through a sterile 0.2 mm membrane filter (13 mm,8 Millipore MILLEX GV) into a sterile assembly comprised of a QC vial connected to a vented dose vial. The total synthesis time was about 38 min from end of beam (EOB).

b. Synthesis using the AutoLoop Module: The loop was loaded with 0.5-0.6 mg of desmethyl P943 in 80-90 mL of anhydrous DMF. [^{11}C]methyl iodide (from MicroLab) was swept through the Loop with helium at 18 mL/min (calibrated for N_2). After activity peaked in the loop, the reaction mixture was allowed to stand at ambient temperature for 5 min and then injected onto the semi-preparative column. The product fraction was collected and diluted with 50 mL de-ionized water, and loaded onto a C18 Sep-Pak. The Sep-Pak was rinsed with 10 mL of 1 mM HCl, and then eluted with 1 mL of USP absolute ethanol followed by 3 mL of saline. The combined eluent was passed through a sterile 0.2 mm membrane filter (33 mm, Millipore MILLEX GV) into a sterile and vented dose vial containing 7 mL saline and 40 mL of 4.2% sodium bicarbonate.

2.2.2. Determination of radiochemical purity and specific activity—The final product was analyzed by radio-HPLC coupled with a gamma detector. A Shimadzu LC-20AT Prominence system was used, which is equipped with a SPD-M20A Diode Array (PDA) detector or SPD-20A UV/Vis detector (254 nm) also operating in series with a Bioscan Flow-Count g-detector. A Jones Genesis C18 4μm 4.6 × 250 mm analytical column was used, eluted under isocratic conditions with mobile-phase system composing of 40:60 (v/v) acetonitrile/0.1 M ammonium formate buffer of pH 4.2 (with acetic acid) and a flow rate of 2 mL/min. The specific activity for [^{11}C]P943 was determined by counting an aliquot in a dose calibrator and determining the mass by HPLC against a calibration curve of the cold standard. Identity was confirmed by a co-injection with the standard.

2.3. Brain PET imaging in non-human primates

PET studies were performed according to a protocol approved by the Yale University Institutional Animal Care and Use Committee (IACUC).

2.3.1. General imaging procedure—PET imaging of the brain distribution of [^{11}C]P943 was carried out in Rhesus monkeys weighing 5-8 kg. Each animal (fasted overnight) received ketamine (10 mg/kg, i.m.) and glycopyrrolate (0.005-0.01 mg/kg, i.m.), and i.v. catheters (infused with normal saline) were inserted in extremity veins for administration of fluids, drugs, and PET radiotracers and for blood sampling. Endotracheal intubation was performed to permit administration of gaseous anesthetics, and isoflurane (∼2% isoflurane) was administered to effect.

The monkey's head was positioned in the tomograph using a custom-designed stereotaxic headholder and was then imaged with a brain-dedicated high-resolution research tomography HRRT (207 slices with 1.2 mm slice separation, resolution ∼ 3 mm FWHM in 3D acquisition mode) PET scanner (Siemens, Knoxville, TN) [20]. The animal was attached to a physiological monitor, and vital signs (pulse rate, blood pressure, respirations, EKG) were continuously monitored. pCO_2 was monitored with an end-tidal monitor, and body temperature with a rectal probe. A transmission scan was obtained before the emission scan for attenuation correction. An average of radioactive dose of 5-7 mCi of [^{11}C]P943 was administered at the time of injection. In studies for which a continuous infusion paradigm was used, a computer-controlled pump (Harvard Instruments) was employed. List mode data were acquired for 120 min duration and reconstructed into dynamic images with a cluster-based iterative reconstruction algorithm [21] with corrections for attenuation, scatter, randoms, deadtime, and decay. Blood samples were drawn to measure the time course of radiotracer and its radioactive metabolites in blood.

2.3.2. Plasma free fraction measurement—The plasma free fraction (f_P) was determined by ultrafiltration of triplicate 0.2-mL aliquots of plasma mixed with the radiotracer. The separation of the protein-bound fraction from the unbound fraction (i.e., free fraction) of the radioactivity in the plasma was achieved by using ultrafiltration tubes (Centrifree UF device number 4104, Millipore, Billerica, MA, USA) and centrifugation (1100g for 20 min; IEC Medilite centrifuge, Thermo Fisher Scientific, Waltham, MA, USA). f_P was calculated as the ratio of the concentration (radioactivity/mL) of the filtrate to that of the total.

2.3.3. Determination of ligand metabolism in plasma—For selected samples (10, 20 40, 60 and 90 min postinjection) plasma proteins were precipitated using acetonitrile (1 mL/mL plasma) and the mixture was centrifuged (14000 g for 4 min; minispin plus centrifuge, Eppendorf, Westbury, NY, USA) to separate the supernatant from the pellet. An aliquot (0.2 mL) of the supernatant was counted in a well-counter and the rest was analyzed by reverse-

phase HPLC. The HPLC system consisted of an isocratic pump (AT-20A, Shimadzu, Kyoto, Japan), an injector (7725i, Rheodyne, Rohnert Park, CA, USA) equipped with a 2 mL sample loop, a C18 Symmetry preparative column (7.8 × 300 mm, 7 μm, Waters, Milford, MA, USA). The column was eluted with acetonitrile and aqueous 50 mM ammonium acetate pH 5.8 (55/45) at a flow rate of 2.8 mL/min. The output of the HPLC column was connected to a fraction collector (CF-1 Fraction Collector, Spectrum Chromatography, Houston, TX, USA). Fractions were collected every minute and counted in a well counter (Wizard, Perkin Elmer). Parent fraction was determined as the ratio of radioactivity in [^{11}C]P943-containing fractions to total injected activity.

2.3.4. Image analysis—Magnetic resonance (MR) images were acquired on each monkey with a 3T scanner to assist with anatomical localization of regions of interest (ROIs). A T1-weighted coronal MRI sequence was used (TE = 3.34, TR = 2530, 176 slices, slice thickness = 0.54 mm, flip angle = 7 degrees, image matrix = 256 × 256, pixel size = 0.5 × 0.5, FOV = 140 mm, 3D turbo flash). The following ROIs were defined on the MR images: caudate, cingulate, occipital, frontal, insula, globus pallidus, putamen and thalamus. Summed PET images were registered to the individual MRIs using a 6-parameter affine mutual information algorithm. To generate each regional time– activity curve (results expressed as KBq/mL), the mean radioactivity in the VOI was calculated for each frame and plotted versus time. For infusion scans at equilibrium, to calculate binding potential (BP_{ND}), the mean concentration from 70-100 minutes in each ROI was divided by the mean concentration during the same time period in the reference region (cerebellum), and a value of one was subtracted from this ratio. BP_{ND} images were calculated in the same way using pixel-by-pixel calculations.

2.4. Experiment design

2.4.1. Baseline study—A 2 hr baseline scan with a bolus injection of [^{11}C]P943 was carried out in one monkey to determine the biodistribution and kinetics of the tracer in the brain. Baseline scans using a bolus injection followed by constant infusion (B/I) paradigm were also performed with bolus component (K_{bol}) of 150 min in a total of four monkeys. The algorithm used to choose an optimum value of K_{bol} has been described previously [22].

2.4.2. Binding saturability study—Six [^{11}C]P943 scans were acquired in 2 different anesthetized rhesus monkeys (a total of 12 scans). For each study day, 3 scans were performed at high, medium, and low specific activities (SA), depending on the amount of unlabeled (cold) P943 added to the injection syringe. Each animal was studied on two days, so six scans were acquired per animal using different levels of SA. All injections were i.v. bolus (2 min) plus constant infusion (118 min) delivered by an automatic pump program. The relative fraction of the dose delivered in the bolus varied for each of the 3 scans (K_{bol} = 150 min for the high SA scans; K_{bol} = 120 for the medium SA scans; K_{bol} = 105 for the low SA scans), since a smaller bolus component is necessary for lower SA scans.

Binding potentials (BP_{ND}) were determined by the equilibrium ratios of the radioactivity concentrations in the ROIs to that in the cerebellum (CER) (minus 1). The saturability of the tracer binding was assessed by comparing the BP_{ND} values between the high SA scan (baseline), and medium and low SA scans (i.e., self-blocking scans) of the tracer binding. Kinetic modeling and estimation of B_{max} (receptor density) and K_d (dissociation constant) will be published elsewhere [23].

2.4.3. Binding selectivity study—The selectivity of [^{11}C]P943 binding towards the 5-HT_{1B} receptor was examined in two rhesus monkeys by blocking with GR127935 (a selective 5-HT_{1B}/5-HT_{1D} antagonist). A control scan was first obtained following a B/I

administration of [^{11}C]P943. GR127935 (2 mg/kg, bolus, iv) was administered 15 min prior to tracer injection in the second scan, in which the same bolus injection plus constant infusion paradigm (K_{bol} = 150 min) was used.

3. Results and discussion

3.1. Chemistry

[^{11}C]P943 contains a piperazine side chain that is common in 5-HT$_{1B}$ antagonists [11]. *N*-Alkylation of the normethylpiperazine moeity of the pyrrolidinone precursor **1** (1-(4-(2-methoxypropan-2-yl)phenyl)-3-(2-(piperazin-1-yl)benzyl)pyrrolidin-2-one) was carried out with [^{11}C]methyl triflate in DMF at 100° C for 4 min (Figure 1, Method A) in the F × C module. The average radiochemical yield was aprox.10% ± 2% at the end of synthesis (based on trapped [^{11}C]methyl triflate) with a specific activity of 326 ± 133 MBq/nmol (8.8 ± 3.6 mCi/nmol) calculated at the end-of-synthesis (n = 37). On the AutoLoop, radiolabeling was accomplished with [^{11}C]methyl iodide at ambient temperature for 5 minutes (Figure 1, Method B); yields and specific activity were slightly lower. Both radiolabeling methods produced [^{11}C]P943 in radiochemical purity of >99%.

3.2. Baseline study

The time-activity curves for a 2 hr baseline scan with a bolus injection of [^{11}C]P943 are presented in Figure 2. The regional uptake of the tracer was shown to be consistent with the known distribution of 5-HT$_{1B}$ receptors in the brain: highest in the globus pallidus and occipital cortex; moderate in other cortical areas, basal ganglia, and thalamus; and lowest in the cerebellum. Peak uptake was reached between 10-30 min in most brain regions with relatively fast kinetics.

In the process of determining the ligand metabolism in plasma, we found the percentage of radioactivity recovered in the supernatant was 96±1% at the beginning of the scan and 92±1% at the end of the scan. The amount of radioactivity in plasma representing unchanged radioligand was 96%, 85%, 71%, 56%, 42%, 32% at 0, 10, 20, 40, 60 and 90 min, respectively (Figure 3, averaged over 25 scans). No lipophilic, labeled metabolite was observed. The mean (n=25) plasma free fraction was ~23%.

Baseline scans using a bolus injection followed by constant infusion (B/I) paradigm were performed in several monkeys with bolus component (K_{bol}) of 150 min (please note: since a smaller bolus component is necessary for lower SA scans, a value of K_{bol} 120 and 105 was applied for the medium and low SA scans, respectively, as shown in Figure 4(A) and 4(B). The mean baseline BP values across regions from a total of 10 baseline scans are presented in Table 2. The time-activity curves for a representative bolus plus infusion baseline scan is presented in Figure 5(A).

3.3. Binding saturability study

Saturability of [^{11}C]P943 binding studies were performed with 3 bolus plus infusion deliveries of [^{11}C]P943 per day on 1-2 days. Specific activity (SA) was varied from 2-200 MBq/nmol (0.05-5 mCi/nmol) by adding various amount of unlabeled (cold) P943. Binding potential (BP_{ND}) was calculated using the equilibrium ratio of regions to cerebellum. Equilibrium was reached by ~70 min (see the time-activity curves for a representative bolus plus infusion baseline scan presented in Figure 5(A), equilibrium was reached by ~70 min in the brain) and data from 70-100 min were used to calculate BP_{ND}. The binding potentials BP_{ND} at high specific activity ranged from 0.25 to 0.75, with the highest values of 0.80 and 0.57 in the occipital cortex and globus pallidus, respectively. The uptake of [^{11}C]P943 in the 5-HT$_{1B}$ receptor rich regions was reduced in a dose-dependent manner by adding various

amount of unlabeled (cold) P943; i.e., self-block (Figure 4A and 4B). Each of the BP_{ND} values presented in the bar graph of Figures 4A and 4B was obtained by averaging the BP_{ND} values from the studies in the two monkeys. These results indicate that the binding of [^{11}C]P943 is saturable.

3.4. Binding selectivity study

A paired study was done in two rhesus monkeys using a constant infusion paradigm. Initially, a control study was performed. Three hours later a second study was performed starting 5 min after i.v. administration of the 5-HT$_{1B}$ antagonist GR127935 (2 mg/kg). Similar mass and activity between the control and blocking scans were injected (i.e., a radioactive dose of 5.4 ± 0.7 mCi of [^{11}C]P943 was administered with a specific activity at time of injection of 6.3 ± 0.9 mCi/nmol for the two pair studies). The time-activity curves for target regions and the reference region (CB) before and after blockade are displayed in Figure 5A and 5B, respectively. The parametric images of binding potentials before and after blockade, along with the corresponding MRI slices, are shown in Figure 6A, 6B, and 6C, respectively. GR127935 resulted in reduction of BP_{ND} values by 42-95% across regions (averaged from two blocking studies in two monkeys) with a near complete displacement of [^{11}C]P943 from the occipital and frontal regions of the brain (reduction of the BP_{ND} values from 0.71 to 0.03 and 0.49 to 0.06 for occipital and frontal cortex, respectively). However, the lack of full blockade in putamen and insula was observed (Table 3). The difference in the calculated % blockade between regions may be due in part to regional variations in the level of nonspecific binding.

4. Discussion

P943 is a 5-HT$_{1B}$ receptor antagonist with physiochemical properties suitable for use as a PET radiotracer. A series of preclinical and clinical assessments performed at Uppsala Imanet, Sweden confirmed that [^{11}C]P943 is a suitable tracer for in vivo evaluations of the 5-HT$_{1B}$ receptor system [15,16]. Here we report the radiolabeling of [^{11}C]P943 that was carried out at the Yale PET Center using automated synthesis modules. Both the GE TRACERLab™ F × C automated synthesizer and Bioscan AutoLoop produced the tracer in high radiochemical yields and with high specific activities.

Our PET studies in rhesus monkeys have shown [^{11}C]P943 to enter the brain readily. The regional pattern in the brain correlates well with autoradiographic determinations: highest uptake in globus pallidus and occipital cortex, areas known to have high concentrations of the 5-HT$_{1B}$ receptor; and a low uptake in the cerebellum, an area known to be devoid of this receptor [24]. The labeled metabolites obtained were more polar (less lipophilic) than the parent tracer, and therefore unlikely to cross the blood-brain barrier and contribute to the brain activity.

It is important to note that a bolus plus constant infusion paradigm was applied to the current tracer evaluation study for [^{11}C]P943. In principle, for reversible ligands, a transient equilibrium can be reached after a bolus injection; however, depending on the rate of plasma clearance and the local tissue kinetics, tissue-to-plasma and tissue-to-reference ratios will be biased. A straightforward approach to eliminate the biases of transient equilibrium measures is to maintain constant blood and tissue concentrations by administering radioactivity as a programmed infusion instead of a bolus. This approach has been used to produce true equilibrium for receptor studies so that V_T and BP can be measured directly and reliably [22]. In this study, we defined the infusion schedule to consist of a combination of bolus and continuous infusion. This infusion paradigm facilitated the quantitative evaluation of [^{11}C]P943, as the equilibrium was reached by ~70 min. Binding potentials (BP_{ND}), can

simply be determined by the equilibrium ratios of ROIs to cerebellum (CER) (minus 1), based on the data from 70-100 min.

The saturability of the tracer binding was supported by a dose-dependent reduction of binding potentials in brain regions by carrying out self-block experiments with the unlabeled parent compound, P943. By adding various amount of cold P943 to the tracer to generate the injection dose with high, medium, and low specific activities, the degree of blocking of the tracer binding to the receptor can then be determined.

Based on the recent literature, the serotonergic system is complex; to date, 14 different serotonin receptors have been distinguished within the serotonin receptor family: 5-HT_{1A}, 5-HT_{1B}, 5-HT_{1D}, 5-HT_{1E}, 5-HT_{1F}, 5-HT_{2A}, 5-HT_{2B}, 5-HT_{2C}, 5-HT_3,5-HT_4, 5-HT_{5A}, 5-HT_{5B}, 5-HT_6, and 5-HT_7[25]. Only recently the 5-HT_{1B} receptor has been distinguished from the 5-HT_{1D} receptor; however, there has been much debate about the nomenclature and classification of the 5-HT_{1B} receptor [26]. The in vitro pharmacology profile for unlabeled P943 is shown in Table 1, demonstrating its potency and selectivity towards 5-HT_{1B}; however, no assay was performed for its selectivity towards 5-HT_{1B} vs. 5-HT_{1D} as there is no drug selective only for 5-HT_{1B} or 5-$HT_{1D.}$ GR 127,935 is a potent and effective antagonist for human 5-HT_{1D} and 5-HT_{1B} with a pKi value of 9.0 and 8.6 for 5HT_{1B} and 5HT_{1D}, respectively [27,28,29]. In our blocking study with GR 127,935, a near complete blockade of [^{11}C]P943 binding was observed after pretreatment with GR 127,935. Due to the lack of available pharmacological tools specifically for 5HT_{1B} and 5HT_{1D} receptor subtypes [30,31], it is difficult to distinguish whether or not [^{11}C]P943 also binds to 5HT_{1D} receptor in vivo. However, in vitro binding assays indicate that binding affinity of P943 is much higher for 5-HT_{1B} than that for 5-HT_{1D} (Table 1). Furthermore, the autoradiograms indicated that the 5-HT_{1B} receptor is much more abundant than the 5-HT_{1D} receptor in the human brain; the latter seeming to occur only in low amounts mainly in the ventral pallidum [32].

The affinity of P943 for 5HT_{1B} is 50-100 times higher than that for 5-HT_{1A} receptors based on the in vitro data (K_i = 62 nM and 1.2 nM for 5-HT_{1A} and 5-$HT_{1B,}$ respectively, based on Table 1; or K_i = 0.77 nM and 85 nM for 5-$HT_{1A\ and}$ 5-$HT_{1B,}$ respectively, based on references 15 and 16). In the human brain, the ratio of 5-HT_{1A} and 5-HT_{1B} receptor concentration varies greatly between brain regions; for example, there are 10 times more 5-HT_{1B} than 5-HT_{1A} receptors in the pallidum, but they are 5 times more 5-HT_{1A} than 5-HT_{1B} receptors in the cortex (using results from Varnäs et al., 2004 [33] & 2005 [31], for the 5-HT_{1B} subtype and Hall et al., 1997 for the 5-HT_{1A} subtype [34]). Since binding potentials are the ratios of B_{max} to K_d, given the relative values of B_{max} and K_d for 5-HT_{1A} and 5-HT_{1B} receptors, the 5-HT_{1A} component of the measured binding potential is expected to be < 10% of the total BP_{ND} in the cortex.

Based on these assessments, our studies demonstrate that [^{11}C]P943 is a suitable PET ligand for imaging 5HT_{1B} receptors.

The results from the preclinical in vitro evaluation study and our in vivo PET imaging studies in non-human primates and humans have been presented as abstracts at several conferences [35a,b,c]. Kinetic modeling methods were recently presented [36a,b]. Recently, a new PET ligand, [^{11}C]AZ10419369 developed by Astra Zeneca Pharmaceuticals also showed promising results [24]. Its selectivity was demonstrated via an in vitro blocking study with the same 5$HT_{1B/1D}$ antagonist GR 127935 used in the present study. It is important to point out that the Astra Zeneca group used only the bolus injection paradigm for their non-human primate studies; however, a bolus plus constant infusion paradigm was applied to the current tracer evaluation study for [^{11}C]P943. Based on the limited results

from the bolus injection paradigm of the two groups, the two tracers appear to have similar brain uptake and similar values for the ratio of the (target) tissue to reference tissue concentration [36(a)]. A careful comparison of [^{11}C]P943 and [^{11}C]AZ10419369 will be facilitated by the publication of modeling studies for both tracers. SB-616234-A (1-[6-(*cis*-3,5-Dimethylpiperazin-1-yl)-2,3-dihydro-5-methoxyindol-1-yl]-1-[20-methyl-40-(5-methyl-1,2,4-oxadiazol-3-yl)biphenyl-4-yl]methanone hydrochloride) also looks promising based on the in vitro and behavior characterization data; however, its in vivo specificity has not been evaluated yet [37, 38].

5. Conclusion

[^{11}C]P943 is a suitable ligand for PET imaging studies of 5HT$_{1B}$ receptors in vivo. This ligand has been advanced to imaging applications in humans and it will be a useful new tracer for studying the functional significance of 5HT$_{1B}$ receptors in humans and its role in various disease states.

Acknowledgments

The authors thank the staff of the Yale University PET Center for their technical expertise and support and Jean-Dominique Gallezot, Ph.D. for helpful discussions. The authors also thank the NIMH Psychoactive Drug Screening Program for the *in vitro* assays of P943. Funding for this study was provided by the Yale Pfizer Bioimaging Alliance. This publication was also made possible by CTSA Grant Number UL1 RR024139 from the National Center for Research Resources (NCRR), a component of the National Institutes of Health (NIH), and NIH roadmap for Medical Research. Its contents are solely the responsibility of the authors and do not necessarily represent the official view of NCRR or NIH.

References

1. Miller HE, Deakin JF, Anderson IM. Effect of acute tryptophan depletion on CO2-induced anxiety in patients with panic disorder and normal volunteers. Br J Psychiatry. 2000; 176:182–8. [PubMed: 10755058]
2. Graeff FG, Guimaraes FS, De Andrade TG, Deakin JF. Role of 5-HT in stress, anxiety, and depression. Pharmacol Biochem Behav. 1996; 54:129–41. [PubMed: 8728550]
3. Zohar J, Mueller EA, Insel TR, Zohar-Kadouch RC, Murphy DL. Serotonergic responsivity in obsessive-compulsive disorder. Comparison of patients and healthy controls. Arch Gen Psychiatry. 1987; 44:946–51. [PubMed: 3675134]
4. Deakin JF, Pennell I, Upadhyaya AJ, Lofthouse R. A neuroendocrine study of 5HT function in depression: evidence for biological mechanisms of endogenous and psychosocial causation. Psychopharmacology (Berl). 1990; 101:85–92. [PubMed: 2343077]
5. Meltzer HY, Li Z, Kaneda Y, Ichikawa J. Serotonin receptors: their key role in drugs to treat schizophrenia. Prog Neuropsychopharmacol Biol Psychiatry. 2003; 27:1159–72. [PubMed: 14642974]
6. Svenningsson P, Chergui K, Rachleff I, Flajolet M, Zhang X, Yacoubi ME, Vaugeois JM, Nomikos GG, Greengard P. Alterations in 5-HT1B receptor function by p11 in depressionlike states. Science. 2006; 311:77–80. [PubMed: 16400147]
7. Engel G, Göthert M, Hoyer D, Schlicker E, Hillenbrand K. Identity of inhibitory presynaptic 5-hydroxytryptamine (5-HT) autoreceptors in the rat brain cortex with 5-HT1B binding sites. Naunyn Schmiedebergs Arch Pharmacol. 1986; 332:1–7. [PubMed: 2936965]
8. Smoller JW, Biederman J, Arbeitman L, Doyle AE, Fagerness J, Perlis RH, Sklar P, Faraone SV. Association between the 5HT1B receptor gene (HTR1B) and the inattentive subtype of ADHD. Biol Psychiatry. 2006; 59:460–7. [PubMed: 16197923]
9. Huang Y, Oquendo MA, Harkavy Friedman JM, Greenhill LL, Brodsky B, Malone KM, Khait V, Mann JJ. Substance abuse disorder and major depression are associated with the human 5-HT1B receptor gene (HTR1B) G861C polymorphism. Neuropsychopharmacology. 2003; 28:163–9. [PubMed: 12496953]

10. Quist JF, Barr CL, Schachar R, Roberts W, Malone M, Tannock R, Basile VS, Beitchman J, Kennedy JL. The serotonin 5-HT1B receptor gene and attention deficit hyperactivity disorder. Mol Psychiatry. 2003; 8:98–102. [PubMed: 12556913]
11. Halazy S, Lamothe M, Jorand-Lebrun C. 5-$HT_{1B/1D}$ antagonists and depression. Exp Opin Ther Patents. 1997; 7:339–352.
12. López-Figueroa AL, Norton CS, López-Figueroa MO, Armellini-Dodel D, Burke S, Akil H, Lopez JF, Watson SJ. Serotonin 5-HT1A, 5-HT1B, and 5-HT2A receptor mRNA expression in subjects with major depression, bipolar disorder, and schizophrenia. Biol Psychiatry. 2004; 55:225–33. Erratum in: Biol Psychiatry 2004;55:660. [PubMed: 14744462]
13. Stenfors C, Hallerbäck T, Larsson LG, Wallsten C, Ross SB. Pharmacology of a novel selective 5-hydroxytryptamine1B receptor antagonist, AR-A000002. Naunyn Schmiedebergs Arch Pharmacol. 2004; 369:330–337. [PubMed: 14758468]
14. Hudzik TJ, Yanek M, Porrey T, Evenden J, Paronis C, Mastrangelo M, Ryan C, Ross S, Stenfors C. Behavioral pharmacology of AR-A000002, a novel, selective 5-hydroxy-tryptamine1B antagonist. J Pharmacol Exp Ther. 2003; 304:1072–1084. [PubMed: 12604684]
15. McCarthy, TJ.; Hoglund, U.; Antoni, G.; Lindhe, O.; Sobolov, S.; Gray, P.; Schaeffer, E.; Poe, R.; Zhang, L.; Bergstrom, M.; Blomqvist, G.; Appel, L.; Langstrom, B. Discovery and qualification of the first selective 5-HT1B PET radiotracer using a novel PET radiotracer development paradigm. Presented at the Joint Molecular Imaging Conference; September 8–11 2007; Providence, Rhode Island, USA. 2007. JMIC Abstract Book, Presentation #0985, p362
16. Helal CJ, Gunnar A, Langstrom B, Sheng JZ, Jaynes-sobolov S, Mccarthy T. 11C-Labeled Benzyl-Lactam Compounds and Their Use as Imaging Agents. United States Patent Application 20080206137 A1.
17. Larsen P, Ulin J, Dahlstrom K, Jensen M. Synthesis of [^{11}C]iodomethane by iodination of [^{11}C]methane. Appl Radiat Isot. 1997; 48:153–7.
18. Jewett D. A simple synthesis of [^{11}C]methyl triflate. Appl Radiat Isot. 1992; 43:1383–5.
19. The silver triflate column was prepared by modifying literature procedure [18]. Briefly, 60 g of graphpac-GC (*Alltech*, uncoated, 80/100) was added to a solution of 25 g of silver trifluromethanesulfonate in 50 mL of anhydrous acetonitrile. The resulting heterogeneous mixture was mixed well and then the solvent was slowly evaporated to dryness.
20. de Jong HW, van Velden FH, Kloet RW, Buijs FL, Boellaard R, Lammertsma AA. Performance evaluation of the ECAT HRRT: an LSO-LYSO double layer high resolution, high sensitivity scanner. Phys Med Biol. 2007; 52:1505–1526. [PubMed: 17301468]
21. Carson, RE.; Barker, WC.; Liow, JS.; Adler, S.; Johnson, CA. Design of a motion-compensation OSEM List-mode Algorithm for Resolution-Recovery Reconstruction of the HRRT Conf Record IEEE Nuclear Science Symposium and Medical Imaging Conference; Portland, OR. 2003; p. M16-6.
22. Carson RE, Channing MA, Blasberg RG, Dunn BB, Cohen RM, Rice KC, Herscovitch P. Comparison of bolus and infusion methods for receptor quantitation: application to [^{18}F]cyclofoxy and positron emission tomography. J Cereb Blood Flow Metab. 1993; 3:24–42. [PubMed: 8380178]
23. Tomasi G, Nabulsi N, Weinzimmera D, Sandiego C, Gallezot JD, Wang E, McLean S, Huang Y, Ding Y, Carson RE. In vivo Scatchard analysis of bolus/infusion 5-HT1B studies with [C-11]P943: Comparison between SR™ and equilibrium methods. Neuroimage. 2008; 41:T16–T16.
24. Pierson ME, Andersson J, Nyberg S, McCarthy DJ, Finnema SJ, Varnäs K, Takano A, Karlsson P, Gulyás B, Medd AM, Lee CM, Powell ME, Heys JR, Potts W, Seneca N, Mrzljak L, Farde L, Halldin C. [11C]AZ10419369: a selective 5-HT1B receptor radioligand suitable for positron emission tomography (PET). Characterization in the primate brain. Neuroimage. 2008; 41:1075–85. [PubMed: 18434202]
25. Olivier B, van Oorschot R. 5-HT1B receptors and aggression: a review. Eur J Pharmacol. 2005; 526:207–217. [PubMed: 16310769]
26. Barnes NM, Sharp TA. Review of central 5-HT receptors and their function. Neuropharmacology. 1999; 38:1083–1152. [PubMed: 10462127]

27. Pauwels PJ, Colpaert FC. Selective antagonism of human 5-HTlD and 5-HT1B receptor-mediated responses in stably transfected C6-glial cells by ketanserin and GR 127,935. European J Pharmacology. 1996; 300:141–145.
28. Rousselle JC, Plantefol M, Fillion MP, Massot O, Pauwels PJ, Fillion G. Specific interaction of 5-HT-moduline with human 5-HT1bas well as 5-HT1dreceptors expressed in transfected cultured cells. Naunyn-Schmiedeberg's Arch Pharmacol. 1998; 358:279–286. [PubMed: 9774213]
29. De Vries P, Willems EW, Heiligers JP, Villalón CM, Saxena PR. Investigation of the role of 5-HT1B and 5-HT1D receptors in the sumatriptan-induced constriction of porcine carotid arteriovenous anastomoses. Br J Pharmacol. 1999; 127:405–12. [PubMed: 10385240]
30. Hoyer D, Hannon JP, Martin GR. Molecular, pharmacological and functional diversity of 5-HT receptors. Pharmacol Biochem Behav. 2002; 71:533–554. [PubMed: 11888546]
31. Varnäs K, Hurd YL, Hall H. Regional expression of 5-HT_{1B} receptor mRNA in the human brain. Synapse. 2005; 56:21–8. [PubMed: 15700286]
32. Varnäs K, Hall H, Bonaventure P, Sedvall G. Autoradiographic mapping of 5-HT_{1B} and 5-HT_{1D} receptors in the post mortem human brain using [3H]GR 125743. Brain Res. 2001; 915:47–57. [PubMed: 11578619]
33. Varnäs K, Halldin C, Hall H. Autoradiographic distribution of serotonin transporters and receptor subtypes in human brain. Hum Brain Mapp. 2004; 22:246–60. [PubMed: 15195291]
34. Hall H, Lundkvist C, Halldin C, Farde L, Pike VW, McCarron JA, Fletcher A, Cliffe IA, Barf T, Wikstrom H, Sedvall G. Autoradiographic localization of 5-HT1A receptors in the postmortem human brain using [3H]WAY-100635 and [11C]way-100635. Brain Res. 1997; 745:96–108. [PubMed: 9037397]
35. (a) [15]. Nabulsi, N.; Huang, Y.; Ropchan, J.; Cosgrove, KP.; Staley, J.; Planta-Wilson, B.; McCarthy, T.; Carson, RE.; Frost, JJ.; Ding, YS. Synthesis and evaluation of [11C]P943 for 5-HT1B receptor studies in primates and humans. Presented at the Joint Molecular Imaging Conference; September 8–11 2007; Providence, Rhode Island, USA. JMIC Abstract Book, Presentation #0155, p74Kim, SH.; Neumeister, A.; Planta-Wilson, B.; Gallezot, JD.; McCarthy, T.; Nabulsi, N.; Huang, Y.; Ropchan, J.; Labaree, D.; Ding, YS.; Carson, RE.; Frost, JJ. High resolution imaging of brain serotonin 5-HT_{1B}receptors using [C-11]943 and the HRRT PET scanner. Presented at the Joint Molecular Imaging Conference; September 8–11 2007; Providence, Rhode Island, USA. JMIC Abstract Book, Presentation #0137, p65
36. (a) Gallezot JD, Nabulsi N, Neumeister A, Planta-Wilson B, Williams WA, Singhal T, Kim S, Maguire RP, McCarthy T, Frost JJ, Huang Y, Ding YS, Carson RE. Kinetic modeling of the serotonin 5 HT1B receptor radioligand [11C]P943 in humans. J Cereb Blood Flow Metab, epub. 2009 in press. (b) Carson RE, Nabulsi N, Weinzimmer D, Sandiego CM, Gallezot JD, Wang E, McLean S, Huang Y, Ding YS. Scatchard analysis of 5-HT_{1B}receptors with [^{11}C]P943 in non-human primates. J Nucl Med. 2007; 49(Suppl 1):79P. [PubMed: 18077526]
37. Scott C, Langmead CJ, Clarke KL, Wyman P, Smith PW, Starr KR, Dawson LA, Price GW, Hagan JJ, Watson J. SB-616234-A (1-[6-(cis-3,5-dimethylpiperazin-1-yl)-2,3-dihydro-5-methoxyindol-1-yl]-1-[2′methyl-4′-(5-methyl-1,2,3-oxadiazol-3-yl)biphenyl-4-yl]methanone hydrochloride): a novel, potent and selective 5-HT1B receptor antagonist. Neuropharmacology. 2006; 50:984–90. [PubMed: 16546225]
38. Dawson LA, Hughes ZA, Starr KR, Storey JD, Bettelini L, Bacchi F, Arban R, Poffe A, Melotto S, Hagan JJ, Price GW. Characterisation of the selective 5-HT1B receptor antagonist SB-616234-A (1-[6-(cis-3,5-dimethylpiperazin-1-yl)-2,3-dihydro-5-methoxyindol-1-yl]-1-[2′-methyl-4′-(5-methyl-1,2,4-oxadiazol-3-yl)biphenyl-4-yl]methanone hydrochloride): in vivo neurochemical and behavioural evidence of anxiolytic/antidepressant activity. Neuropharmacology. 2006; 50:975–83. [PubMed: 16581092]

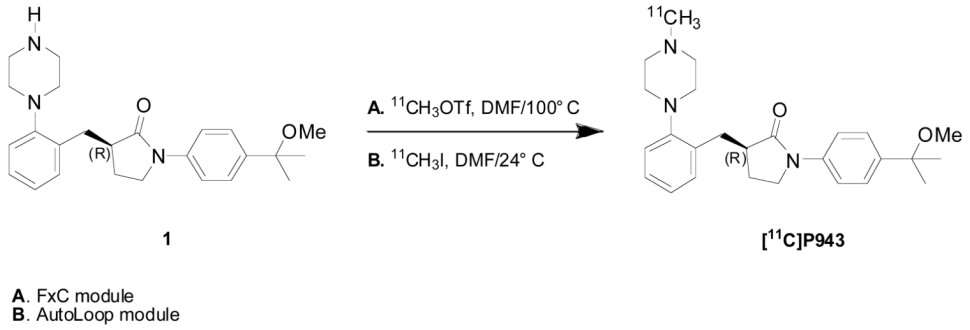

Figure 1.
Radiosynthesis of [^{11}C]P943 via the automated FxC module (method A) and the AutoLoop (method B).

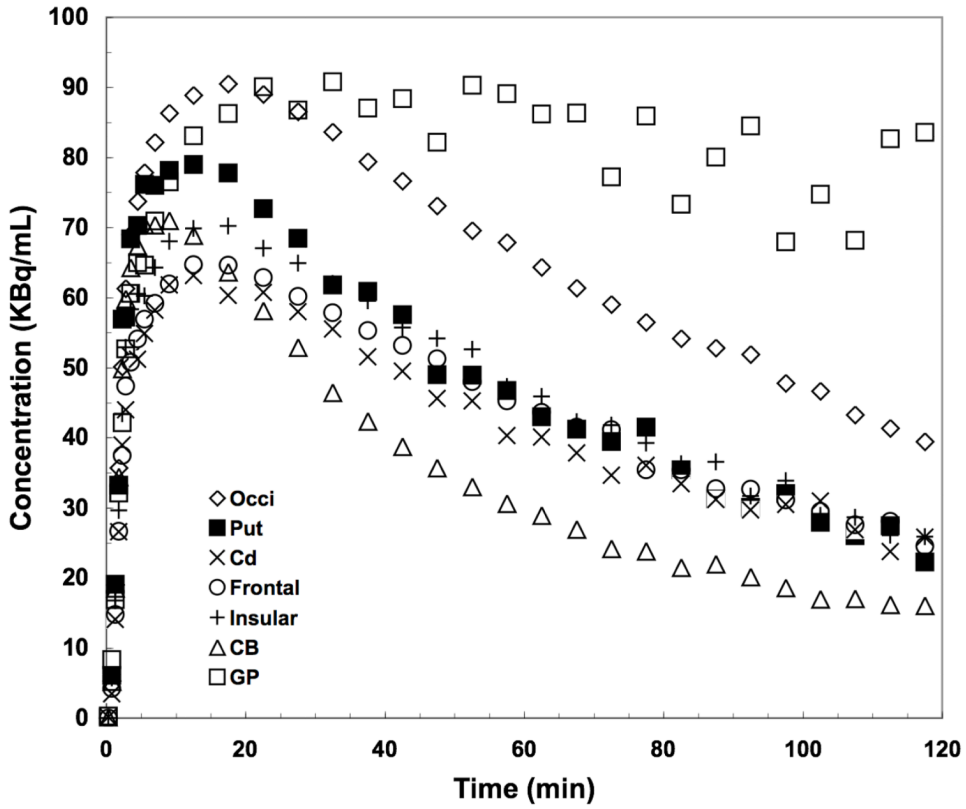

Figure 2.
Time-activity curves after a bolus injection of [^{11}C]P943 for occipital cortex (Occi), putamen (Put), caudate (Cd), frontal and insular cortex, cerebellum (CB) and globus pallidus (GP).

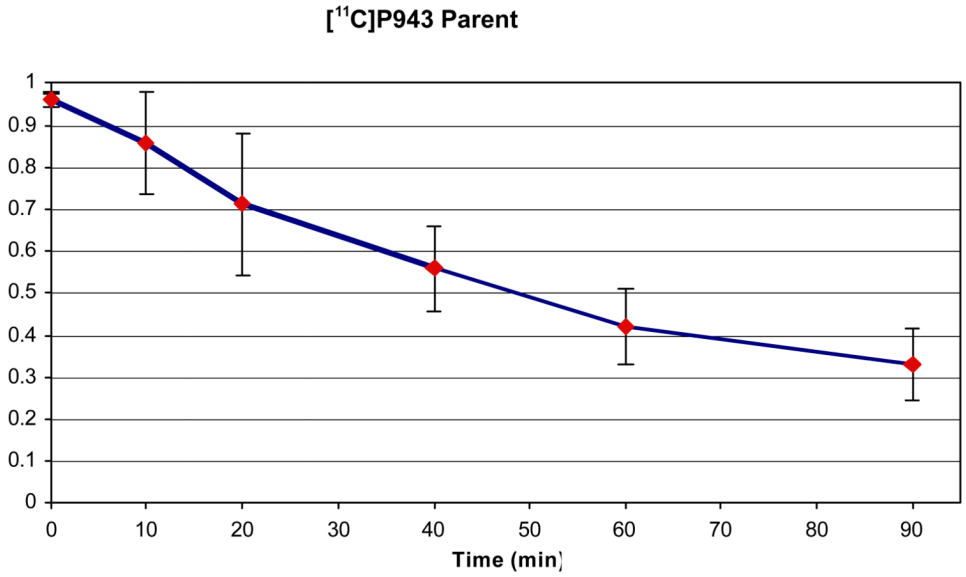

Figure 3.
[^{11}C]P943 parent fractions in the plasma at various time points (averaged over 23 scans).

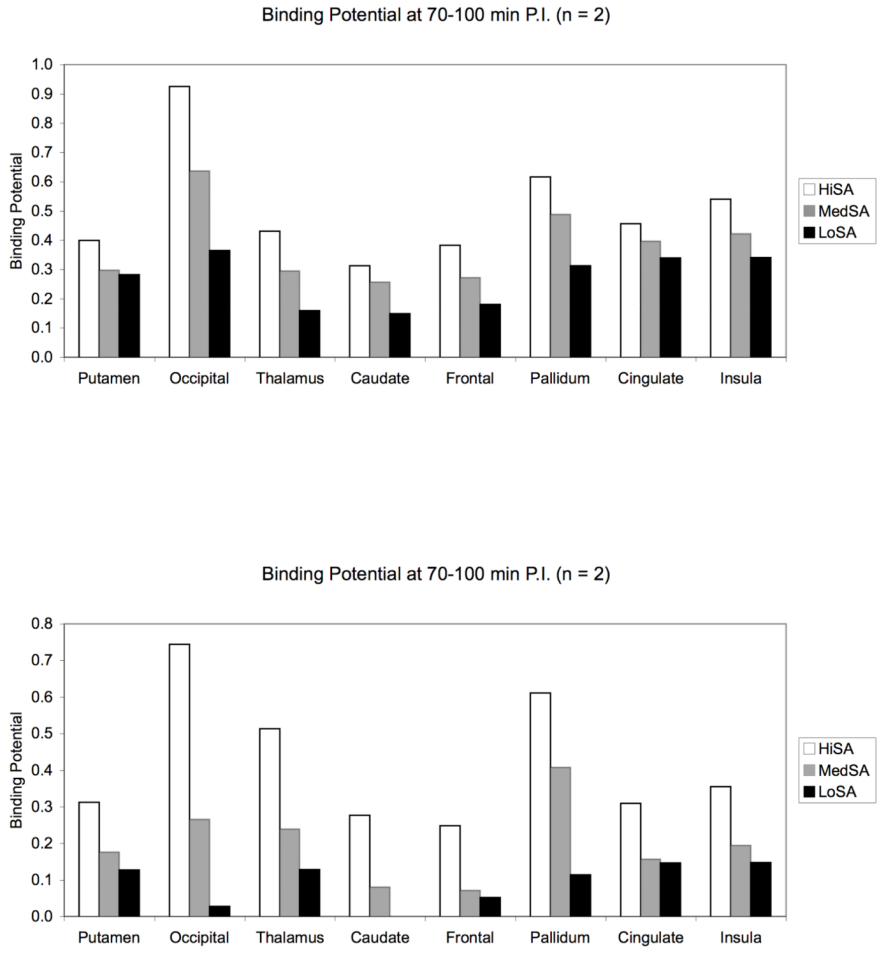

Figure 4.

Binding potentials (BP_{ND}) of [^{11}C]P943 at different levels of specific activity (SA) by adding various amount of unlabeled (cold) P943. All values shown are averages from n = 2 studies. (A) HiSA = no cold added; MedSA = 2 nmol/kg/hr added; LoSA = 8 nmol/kg/hr added. The net specific activities for HiSA, MedSA and LoSA at the time of injection are 118.6, 7.37, 1.88 MBq/nmol, respectively; (B) HiSA = no cold added; MedSA = 6 nmol/kg/hr added; LoSA = 25 nmol/kg/hr added. The net specific activities for HiSA, MedSA and LoSA at the time of injection are 111.7, 2.25, 0.62 MBq/nmol, respectively.

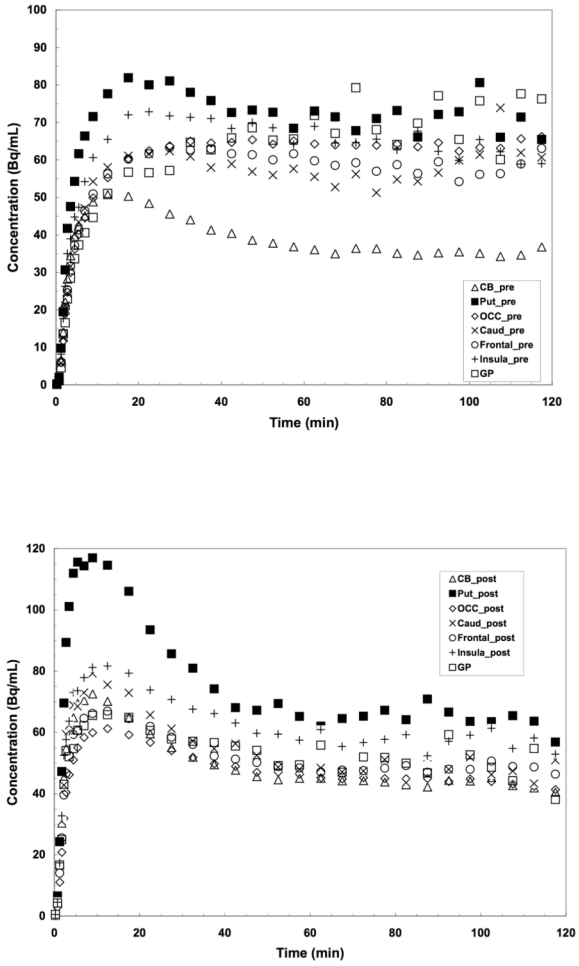

Figure 5.

Time-activity curves for putamen (Put), occipital cortex (Occi), caudate (Cd), frontal cortex, insula, and the reference region (cerebellum, CB): (A) represents control data points (scan 1); (B) represents data points after blockade with 2 mg//kg of GR127935 (scan 2).

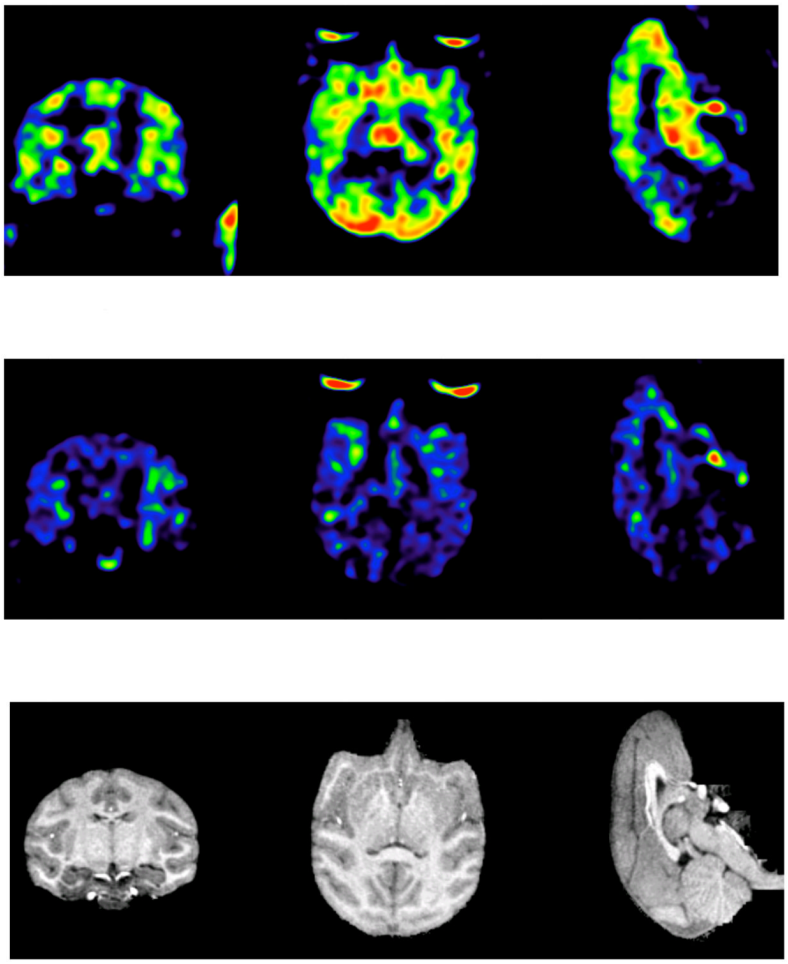

Figure 6.
Parametric images of BP_{ND} derived from images summed from 70 to 100 minutes post-injection (A) at baseline (injected dose: 4.85 mCi) and (B) after preblock with the $5HT_{1B}$ receptor antagonist GR127935 (injected dose: 6.46 mCi). Both studies were carried out for 120 min using isoflurane (2%) as the anesthetic agent; (C) corresponding MRI slices are displayed for anatomical reference. Brain regions with the highest BP_{ND} of [^{11}C]P943 are shown in red, with progressively lower concentrations displayed in yellow, green, and blue, respectively. Images were smoothed using 2x2x2 mm Gaussian kernel.

Table 1

***In vitro* pharmacology profile for unlabeled P943**

P943 Binding Data Ki (nM) from the NIMH Psychoactive Drug Screening Program							
5-HT_{1A}	5-HT_{1B}	5-HT_{1D}	5-HT_{2A}	5-HT_{2B}	5-HT_{2C}	5-HT_{3}	5-HT_{7}
62	1.2	12	2,217	7,102	5,117	157	5,586

Table 2

Baseline binding potential (BP_{ND}) values* across regions (n = 10)

BP_{ND}	Putamen	Occipital	Thalamus	Caudate	Frontal	Globus Pallidus	Cingulate	Insula
MEAN	0.44	0.71	0.44	0.29	0.38	0.60	0.50	0.51
SD**	0.21	0.25	0.09	0.11	0.11	0.20	0.13	0.14

* BP_{ND} was calculated by the mean concentration from 70-100 minutes in each ROI divided by the mean concentration during the same time period in the reference region (cerebellum), and a value of one was subtracted from this ratio. The mean baseline BP_{ND} values across regions were derived from a total of 10 baseline scans using the bolus plus infusion paradigm.

** standard deviation from the mean values.

Table 3

GR127935 blocking study* (n = 2)

%Reduction in BP_{ND}	Putamen	Occipital	Thalamus	Caudate	Frontal	Globus Pallidus	Cingulate	Insula
Monkey#1	47	96	76	78	84	80	66	61
Monkey#2	33	94	74	45	98	66	61	45
Mean	40	95	75	62	91	73	64	53

*A paired study (baseline study followed by a blocking study with three hour separation of injections) was performed in two rhesus monkeys using a constant infusion paradigm. The 5-HT_{1B} antagonist GR127935 (2 mg/kg, i.v.) was administered 5 min prior to the beginning of the 2nd tracer injection.